On the crystal and magnetic ordering structures of clinoatacamite, γ-Cu$_2$(OD)$_3$Cl, a proposed valence bond solid

FAST TRACK COMMUNICATION

On the crystal and magnetic ordering structures of clinoatacamite, γ-Cu$_2$(OD)$_3$Cl, a proposed valence bond solid

A S Wills[1,2,4] and J-Y Henry[3]

[1] Department of Chemistry, University College London, 20 Gordon Street,
London WC1H 0AJ, UK
[2] The London Centre for Nanotechnology, 17-19 Gordon Street, London WC1H 0AH, UK
[3] Commissariat à l'Energie Atomique, DSM/DRFMC/SPSMS, 38054 Grenoble, France

E-mail: a.s.wills@ucl.ac.uk

Abstract
Frustrated magnetic systems provide routes to exploring degeneracies and creating new
electronic states. While there has been extensive theoretical study concerning the effects in the
$S = 1/2$ quantum limit, little is known experimentally because of the scarcity of model
materials, in particular systems with the pyrochlore and kagomé lattices of corner-sharing
tetrahedra and triangles, respectively. Much interest has developed from the discovery of
herbertsmithite, ZnCu$_3$(OH)$_6$Cl$_2$, a material for which magnetic order has not yet been found,
and its proposal as a model $S = 1/2$ kagomé antiferromagnet. This work reopened the debate
over the nature of the ground state for this archetypal quantum magnet and had led to recent
theoretical suggestions that resonance effects, similar to those used to explain aromaticity in
benzene, crystallize an exotic localized spin structure called a valence bond solid (VBS) from
the quantum spin liquid phase.

Inspired by the work on herbertsmithite, studies of the parent material clinoatacamite,
γ-Cu$_2$(OH)$_3$Cl, in which the kagomé layers, that are separated by Zn^{2+} in herbertsmithite, are
coupled by Cu^{2+} ions have led to suggestions that the exchange interactions connecting these
spins to those in the kagomé layers are only weak, which allows a transition to occur at
$T \sim 18$ K to a VBS, made up of singlets formed from the dimerized spins of the kagomé
planes. We present neutron diffraction studies of the crystallographic and magnetic structures
that cast doubt on this interpretation and instead indicate significant coupling of all the
Cu spins. Further, we find that the low temperature transition is associated with a canted
ferromagnetic structure which is incompatible with the VBS.

(Some figures in this article are in colour only in the electronic version)

1. Introduction

Interactions are frustrated when a competition exists that
prevents them from being minimized individually. This
typically leads to degeneracies and highly-correlated dynamics.

While frustration is a general concept, much of the pioneering
work into its consequences continues to be done on
magnetic systems due to their relative simplicity [1]. In both
experimental and theoretical magnetic models, frustration has
been found to lead to new types of magnetic ground states,
and new drives for magnetic ordering. Particular interest is

[4] Author to whom any correspondence should be addressed.

focused on frustrated kagomé and pyrochlore magnets as the low connectivity leads to very large degeneracies, enhancing the effects of frustration.

Experimentally, a large range of exotic ground states has been found in model geometrically frustrated systems. A far from exhaustive list includes the spin liquid states of the insulator $SrCr_{9p}Ga_{12-9p}O_{19}$ (SCGO) [2] and the itinerant magnet YMn_2 [3, 4], the topological spin glass state of $(H_3O)Fe_3(SO_4)_2(OH)_6$ [5], the spin ice states of $Dy_2Ti_2O_7$ and $Ho_2Ti_2O_7$ [6], and the partial ordering of the spins in $Gd_2Ti_2O_7$ [7]. Such is the complexity of frustrated physics that it is notable when a predicted structure is found, e.g. the ground state for a pyrochlore antiferromagnet with dipolar interactions [8] in $Gd_2Sn_2O_7$ [9] and fluctuation stabilized order in $Er_2Ti_2O_7$ [10].

As well as causing exotic magnetic orderings, frustration can have a profound influence on the ordering process. It may allow relatively weak energy scales: such as the Dzyaloshinsky Moriya (DM) interaction [11] or spin anisotropy to drive the fluctuating paramagnetic state to order, e.g., the jarosites [12], or to stabilize long-ranged order that coexists with emergent excitations, e.g. $ZnCr_2O_4$ [13]. This balance of energy scales can also create systems that are on the verge of magnetic order, e.g. gadolinium gallium garnet (GGG) [14] and β-Mn, [15], $Y_{1-x}Sc_xMn_2$ [4], $(H_3O)(Fe_{3-x}Al_x)(SO_4)_2(OH)_6$ [16], or $Tb_2Ti_2O_7$ [17], where the control of the magnetic order can be achieved by chemistry or pressure. Recently, a new field of opportunities has been beautifully demonstrated by the micro-fabrication of the artificial pyrochlore-like [18] and kagomé [19, 20] spin ices.

Long standing goals for experimentalists are the discovery of model kagomé and pyrochlore magnets with which to explore frustration in the quantum limit. Recently, herbertsmithite, $ZnCu_3(OH)_6Cl_2$ [21], was identified in which preferential substitution of the Cu^{2+} sites by Zn^{2+} in the distorted pyrochlore clinoatacamite, γ-$Cu_2(OH)_3Cl$, leads to a magnet with well separated kagomé layers [21]. To date no magnetic transition has been found in herbertsmithite and its low temperature physics remain unclear, but the structural relationship with clinoatacamite, which does show a long range order, allows chemical control of the frustrated quantum ground state [22].

Early studies by Wills and Raymond of clinoatacamite using bulk susceptibility and specific heat showed that the strong exchange, $\theta_{CW} \leqslant 180$ K, was highly frustrated with sequential ordering transitions occurring at 6.1 and 5.8 K [23]. The low value of the released entropy, only $\sim 25\%$ of that expected for a $S = \frac{1}{2}$ system, was evidence for extensive quantum fluctuations. The low temperature specific heat was modeled by thermal activation across a gap of $\delta \sim 1.2$ meV that could be observed as a dispersion-less mode in the inelastic neutron scattering spectra. Later specific heat studies revealed the presence of another transition, at $T \sim 18$ K below which static components could be seen in the MuSR spectra [24, 25]. The nature of this phase transition remains unclear as the ordered component associated with this transition appears to be very small: with only a small feature being observed in the specific heat [24] and no clear signature being seen in

the neutron scattering spectra. Recently, Lee *et al* proposed that the elastic and inelastic neutron scattering spectra are compatible with the formation of a valence bond solid (VBS) at 18 K that survives the formation of collinear magnetic order at ~ 6 K. This suggestion was remarkable as it provided direct experimental evidence of the VBS state being preferred over a quantum spin liquid state at high temperatures, and the impact that localized resonance terms can have in emergent quantum phases [26–30]. Central to their arguments was the proposal that the exchange geometry leads to a reduction in the effective dimensionality of the magnetic system from a 3D distorted pyrochlore to being one of decoupled kagomé planes [25]: a situation reminiscent of $Li_2Mn_2O_4$ [31] and the spinel series $Li_xMn_2O_4$ [32].

We report a neutron diffraction study of the crystal structure of clinoatacamite. It shows that the magnetic superexchange geometry is not as required for the VBS model. Our studies also indicate that rather than being collinear, the magnetic structure at 2 K is canted and weakly ferromagnetic, suggesting that a DM component is involved in the $T \sim 6$ K transition.

2. Method

5 g of deuterated γ-$Cu_2(OD)_3Cl$ powder were prepared from D_2O and anhydrous $CuCl_2$, obtained from dehydration of $CuCl_2 \cdot 2H_2O$. The reaction took place in a PTFE-lined autoclave that was heated at 180 °C for 48 h then cooled at 2° h^{-1} to 120 °C before being rapidly cooled to room temperature. The vessel was rotated about its horizontal axis to prevent sedimentation. Powder x-ray diffraction showed no atacamite impurity, the dominant product of synthesis at $T < 60$ °C.

Diffraction data were collected with neutrons of wave-length 1.594 Å using the D2b diffractometer at the ILL. Approximately 2 g of sample was held in a 10 mm diameter vanadium can with temperature being controlled using an 'Orange' cryostat. Data were taken during both above ($T = 10$ K) and below ($T = 2$ K) the Néel ordering temperature, $T \sim 6$ K. Analysis of the crystal structure was carried out using data over the entire angular range ($8° \leqslant 2\theta \leqslant 130°$) using GSAS [33]. The experimental and calculated diffraction spectra are shown in figure 1. Bond valence calculations were carried out using VaList [34]. While the magnetic phase was included in the refinement the relative weakness of the magnetic scattering prevent it from contributing significantly. The averaged structure of clinoatacamite is low symmetry due to the presence of a cooperative Jahn–Teller effect. Described in the space group $P \, 1 \, 2_1 \, n \, 1$ (14b:2), the Cu ions occupy three distinct crystallographic sites: Cu1: (0.2413, 0.7656, 0.25141); Cu2: (0.5, 0, 0); Cu3: (0, 0, 0). The Cu1 ions form chains parallel to the b-axis, while the Cu2 and Cu3 alternate to form chains parallel to the a-axis. The positions of the deuteriums had not been previously identified and were determined initially from difference Fourier maps and subsequently refined. There was no evidence of proton substitution for deuterium and the refined site occupancies were all set at unity. The refined structure is in good agreement
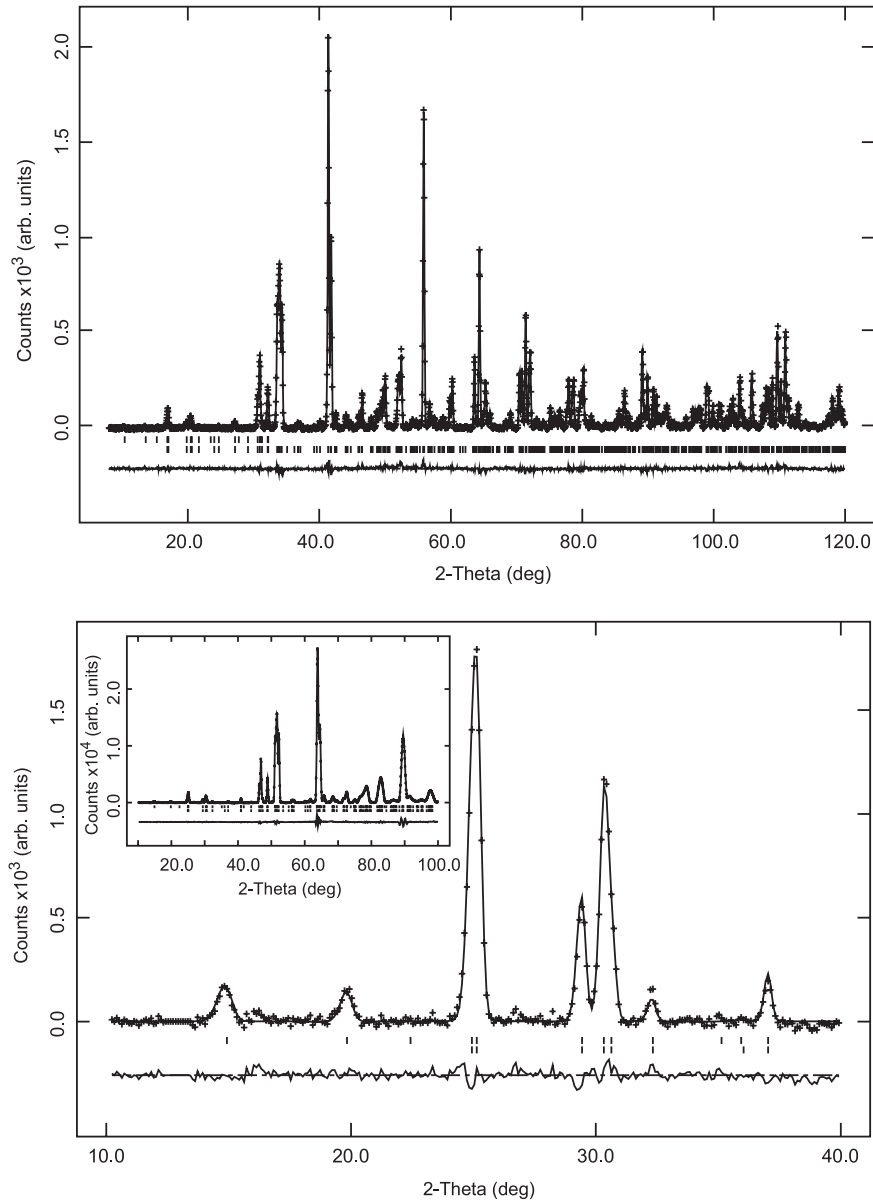
Figure 1. Fit to the powder neutron diffraction pattern of γ-Cu$_2$(OD)$_3$Cl. The upper tick marks indicate the predicted locations of the magnetic scattering, the lower to those of the nuclear phase. The crosses correspond to the observed scattering, the line to the calculated diffraction pattern of the nuclear phase and the difference is shown below. (Top) Data collected 2 K using with the diffractometer D2b and neutrons of wavelength 1.594 Å. The final goodness of fit parameters were $\chi^2 = 2.398$ and $R_{wp} = 0.0441$ with 46 refined parameters. (Bottom) Using data collected with the diffractometer D20 and neutrons of wavelength 2.41 Å. The main panel shows the low angle region where there is appreciable magnetic scattering, and the inset the complete data and fit. The final goodness of fit parameters are $\chi^2 = 343.9$, $R_{wp} = 0.0286$ with 15 refined parameters.

with that of Oswald and Guentier [35] and the refined parameters are given in table A.1. Selected crystal structure information including the individual bond valences, bond valence sums and bond angles related to the superexchange are given in tables A.2 and A.3.

3. Crystal structure of γ-Cu$_2$(OD)$_3$Cl and magnetic superexchange

Figure 2 shows the crystal structure with the kagomé planes formed from Cu1 and Cu2 highlighted by its orientation. The cornerstone of the proposed VBS state are suggestions that the coupling between these layers is weak as the

Cu1–O–Cu3 and Cu2–O–Cu3 bridging angles are close to 95° [22]. This argument comes from work on Cu–O chain systems where the superexchange between Cu^{2+} ions mediated through the oxygen p$_x$ and p$_y$ orbitals changes from ferromagnetic to antiferromagnetic at a Cu–O–Cu bridging angle of 95° [36, 37]. The superexchange geometry in these chains is, however, unlike that found in clinoatacamite where the oxygen bridges three copper centers and bonds to the hydrogen (deuterium) to form a bridging μ_3-OH (figures 2 and 3). The bond lengths and angles in clinoatacamite indicate that the hybridization of the oxygen is between sp^2 and sp^3 and we describe it as sp^{2+x}, where $x < 1$.

3
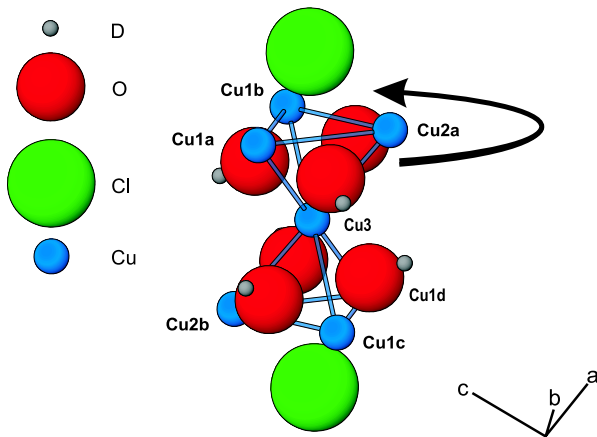
Figure 2. The crystal structure of γ-$Cu_2(OD)_3Cl$ refined at 2 K using neutron diffraction data collected with the diffractometer D2b using 1.594 Å shown to highlight the geometry of the bonding that couples the kagomé planes made up of Cu1 and Cu2. The deuterium positions are show. The labeling scheme and the direction indicated by the arrow define those used in figure 3.

When considering the distortions of the μ_3-OH away from the tetrahedral geometry it is useful to look at Cu^{2+} ions bridged by OH^- ions in the μ_2 and μ_3 limits. DFT calculations for Cu–(μ_2-OH)–Cu bridging angles, ϕ, between 90° and 130° showed that for angles below ~120° the exchange is ferromagnetic, with a maximum amplitude at $\phi \sim 103°$, and antiferromagnetic for $\phi > 120°$, becoming more antiferromagnetic as ϕ increases [38]. In several cubanes with the core $[Cu_4(\mu_3\text{-OH})_4]$ this changeover of coupling sign occurs at angles of approximately 101°–105° [39, 40]. Given the range of values of ϕ observed in clinoatacamite, 91° < ϕ < 102°, and the high connectivity of the pyrochlore-type lattice an appreciable degree of ferromagnetic coupling is expected to be present, competing with the antiferromagnetic exchange.

The breakdown of the equivalence between the four spins of the symmetric tetrahedra into distorted tetrahedra built up of 2 × Cu1, 1 × Cu2 and 1 × Cu3 spins, suggests that the intrinsic symmetry of the clinoatacamite magnetic lattice is one of approximately perpendicular chains that are coupled

by a range of frustrated magnetic interactions. There is little evidence to suggest that the Cu3 spins are decoupled from the Cu1 and Cu2 spins. It is not possible to say more without detailed electronic structure calculations or spin wave data.

4. Symmetry adapted magnetic orderings

High quality magnetic neutron powder diffraction spectra were obtained using the high flux D20 diffractometer also at the ILL using with wavelengths of 2.41 Å. The only distinct magnetic peaks were the (001) and (010), at 15.0° and 19.9° respectively, indicating that the propagation vector for the magnetic structure is $\bar{k} = (000)$. Subtractions made from data collected at 3 K and at 10 K revealed the presence of weak but significant magnetic contributions to several other reflections. To make the most of these data, refinement of the magnetic and nuclear phases was carried out with data over the range 10° ⩽ 2θ ⩽ 100°. The atomic positions of the nuclear phase were fixed at those refined from the D2b data.

Symmetry analysis of the different possible magnetic structures was performed using SARA*h* [41, 42]. In this case, with the propagation vector $\mathbf{k}_7 = (0, 0, 0)$, in Kovalev's notation [43], all of the corepresentations for the four one-dimensional representations of the little group $G_k = G_0 = P\,1\,2_1\,n\,1$, are identical to the representations [45, 46]. Further, as the inclusion of the antiunitary symmetry and the construction of the corepresentations does not bring with it any new information, we will use the more common description in terms of representations (IRs) [47].

The decompositions of the magnetic representation and the basis vectors for the different atomic positions are given in tables B.1 and B.2. If the assumption is made that the ordering at 6 K involves components of the three Cu sites (while the ordering process as ~6 K is sequential there is no evidence to suggest that this is not the case), then the common IRs (Γ_1 and Γ_3) are expected to describe the resulting magnetic structure. The basis vectors of these IRs are similar for the three Cu sites: in Γ_1 the components of the moments in the ac plane are compensated and the components parallel to the b-axis are uncompensated; Γ_4 is the converse, i.e. the components
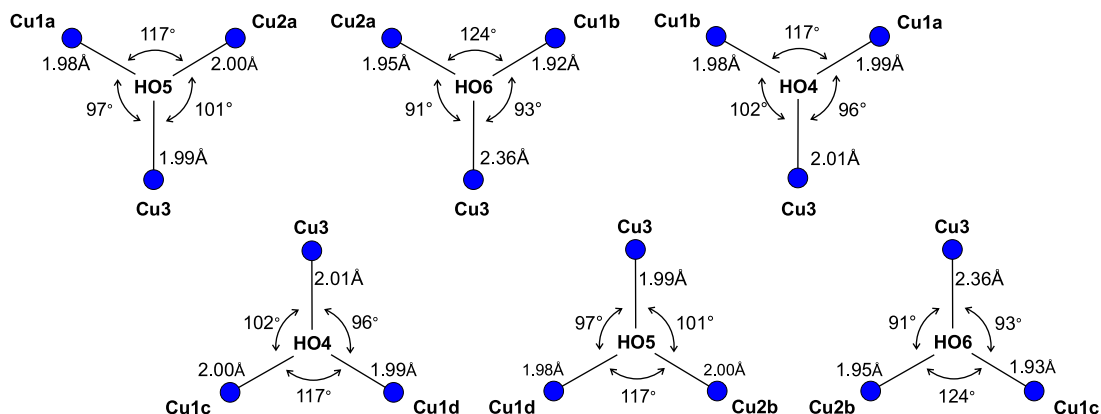
Figure 3. A schematic of the μ_3-OH bonding geometries for the different triangular faces of the tetrahedra shown in figure 2 following the order indicated by the arrow. The labeling scheme is defined in the same figure. The values given are for the adjacent Cu–O–Cu bond angle and for the Cu–O bond length. The electronic configuration of the oxygen is between sp^2 and sp^3.

parallel to a and c are ferromagnetically aligned, and those parallel to b are antiferromagnetically aligned.

Analysis of the magnetic neutron diffraction data was carried out using SARA*h* together with GSAS. The orientations of the magnetic moments, Ψ, within a symmetry type are defined by a linear combination of the basis vectors ψ_i, $\Psi = \sum_i C_i \psi(i)$, where C_i is a weighting coefficient. The moment sizes were refined using least squares algorithms within GSAS and constrained according to a number of models that will be detailed below. The refinements of the weighting coefficients were found to converge within 200 reverse-Monte Carlo technique cycles, with four least squares cycles allowed to refine the sizes of the moments. Refinements of a given set of basis vectors were repeated five times to verify that the refinement had indeed reached its best minimum and which features of the refined structures may be considered robust.

Fits of the D20 diffraction neutron data to model structures associated with these symmetries were examined sequentially. Initial refinements indicated that structures based on Γ_3 were unable to match the intensities of all of the observed reflections well, and that the data could only be well fitted by Γ_1. Different basis vector combinations within this symmetry type were examined subsequently.

The limited information contained in the weak magnetic power diffraction data and the crystallographic similarities of the Cu2 and Cu3 sites, they have the same Wyckoff symmetry, leads to correlation between their refined moments. To stabilize the refinement two limiting models were examined: one where the contribution of Cu3 was null, as proposed by Lee; and one in which the mixing coefficients of Cu2 and Cu3, for a given basis vector index, were constrained to have the same magnitude and their phases, whether ferromagnetic or antiferromagnetic, were refined. The presence of a component parallel to the b axis did not improve the refinements and was subsequently excluded. The refinement was therefore restricted to the mixing coefficients C_{ψ_1} and C_{ψ_3} for the each of the three copper sites.

The magnetic structures of the best fits to the low temperature diffraction data all share common features: on a given tetrahedra the pair of moments that correspond to Cu1 are antiparallel in the ac plane, and canted significantly away from the a-axis; the moments Cu2 and Cu3 are parallel. There however is an uncertainty about whether the Cu2 and Cu3 moments are along the a-axis or canted away from it, as the data can be well fitted with the Cu2 and Cu3 moments restricted to lie parallel to the a-axis. The refined structure is shown in figure 4. Refined values of the moments on the Cu1 sites are 0.58 μ_B, and on the Cu2 and Cu3 sites 0.57 μ_B.

Models suggested by Lee *et al* [13] in which the moments of Cu1 and Cu2 are equal, and those of Cu3 are zero were also examined. Restriction of the refinement to models in which the moments were restricted to be in the ac plane led to a significant worsening of the refinement ($\chi^2 = 350.6$, $R_{wp} = 0.0289$). Fixing the moments on the Cu1 and Cu2 sites to be collinear, further worsened the quality of the refinement ($\chi^2 = 351.8$, $R_{wp} = 0.0290$).
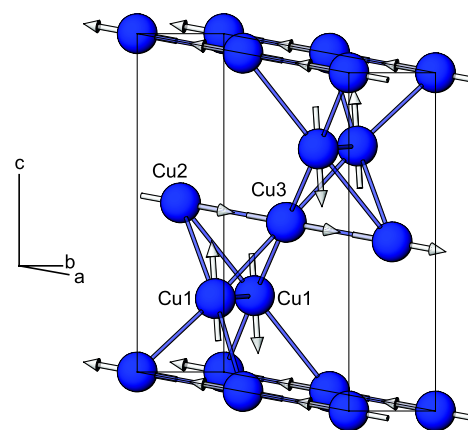
Figure 4. The refined magnetic structure of γ-Cu$_2$(OD)$_3$Cl at 3 K. The angle between the Cu1 spins and the a-axis is not well defined. A small canting parallel to the b-axis is compatible with the weak ferromagnetism observed in [25].

5. Discussion

Our study of the crystal structure and the superexchange paths in clinoatacamite indicate that the magnetic system is not well described by the model of weakly coupled kagomé planes that forms the basis of the VBS model of Lee *et al*. Instead, the μ_3-nature of the bridging hydroxide links together the three types of copper ions to form a three-dimensional network. Clinoatacamite is therefore best considered as a distorted quantum pyrochlore built up of nearly perpendicular chains, as proposed earlier [23].

In light of the weakness of the magnetic scattering and the lack of detailed information about the exchange, it is not possible for powder neutron diffraction to yield a conclusive model for the Néel structure below $\sim$6 K, beyond its symmetry, which corresponds to the irreducible representation Γ_1. While the apparent absence of the (100) reflection suggests that the moments are collinear with the a-axis, the presence of 8 Cu moments in the unit cell means that other spin structures could also lead to this reflection being too weak to be observed. Also, the nature of the magnetic transitions at 6 K need to be taken into account, bulk measurements indicate that below these transitions there is a hysteresis indicative of a ferromagnetic component. The observed increase in the transition temperature with the application of an external magnetic field [24] suggests that the field is suppressing the rapid fluctuations and moving the balance towards long range order. Inspection of the basis vectors associated with Γ_1 suggest that a DM component could give rise to a ferromagnetic moment along the b-axis that would be enhanced by coupling to an external magnetic field. The ordering process at 6 K may therefore be related to the DM component, or similar single-ion component, breaking some of the degeneracies of this frustrated system that survive the first transition at 18 K. The complex nature of this higher temperature phase transitions remains unclear—as yet there is no significant observed change in the inelastic neutron scattering spectra, but the small change in magnetic entropy does suggest that it is a direct consequence of the frustration

of the pyrochlore lattice surviving the low symmetry of the exchange structure.

Since the submission of this manuscript an alternative study of the low temperature magnetic ordering in clinoatacamite has been published in [48]. In their refinement the moments have been constrained to be collinear in the ac plane and allowed to cant along the b-axis, rather than being allowed to refine according to the symmetries expected for the positions themselves. In our refinements we found that such restrictions worsen the quality of the fit and therefore appear unlikely. Some degree of caution must also be expressed over the accuracy of the calculated superexchange integrals, as the details of the magnetic exchange will be critically dependent on the angle of the OH group and the proton (deuterium) positions were not known prior to our work.

In conclusion, our studies of the crystallographic and magnetic structures of clinoatacamite, suggest that a large degree of frustration survives the low symmetry of the exchange geometry. These indicate that the low temperature transition is related to a canted ferromagnetic component that appears incompatible with the proposal that the Cu^{2+} spins condense into a VBS. This study, therefore, negates key experimental evidence in support of the VBS in clinoatacamite and reopens the highly controversial debate over the nature of the ground state of the quintessential frustrated magnet, the $S = 1/2$ kagomé antiferromagnet.

Acknowledgments

Appendix A. Crystal structure information

Table A.1. The crystallographic parameters for γ-$Cu_2(OD)_3Cl$ at 2 K in the space group $P\,1\,2_1\,n\,1$ (14b:2). The refined lattice parameters are $a = 6.151\,75(8)$ Å, $b = 6.816\,06(9)$ Å, $c = 9.105\,41(13)$ Å, and $\beta = 99.8394(11)°$. $R_{WP} = 0.0441$ and $\chi^2 = 0.0441$ for 46 variables.

Atom name	X	Y	Z	U_{iso}
Cu1	0.241 3(4)	0.765 6(4)	0.251 41(32)	0.011 82(28)
Cu2	0.500 000	1.000 000	0.000 000	0.011 82(28)
Cu3	0.000 000	1.000 000	0.000 000	0.011 82(28)
O4	0.079 4(4)	1.019 2(4)	0.223 45(25)	0.012 48(22)
O5	0.259 0(4)	0.820 4(4)	0.039 72(33)	0.012 48(22)
O6	0.309 7(4)	0.209 2(4)	0.049 64(33)	0.012 48(22)
Cl7	0.611 99(20)	0.995 59(32)	0.307 33(14)	0.012 48(22)
D8	0.720 18(40)	0.685 4(4)	0.021 34(35)	0.022 8(4)
D9	0.761 53(43)	0.292 0(4)	0.027 39(35)	0.022 8(4)
D10	0.552 73(34)	0.522 0(5)	0.230 68(25)	0.022 8(4)

Table A.2. Selected bond lengths for γ-$Cu_2(OD)_3Cl$ at 2 K. The bond valence contributions for each bond, s_{ij} and the bond valence sum, $\sum s_{ij}$, are given for each Cu ion [34]. The latter are in good agreement with the expectations for Cu(II). Bonds that do not have well defined set of bond valence parameters are indicates by '—'.

Bond	Bond length (Å)	Oxidn. state assumed	s_{ij}
Cu1–O4	1.99	Cu(2)	0.431
Cu1–O4	2.001	Cu(2)	0.419
Cu1–O5	1.984	Cu(2)	0.439
Cu1–O6	1.929	Cu(2)	0.509
Cu1–Cl7	2.742	Cu(2)	0.135
Cu1–Cl7	2.829	Cu(2)	0.106
$\sum s_{ij}$			2.039
Cu2–O5	2.003	Cu(2)	0.417
Cu2–O5	2.003	Cu(2)	0.417
Cu2–O6	1.947	Cu(2)	0.485
Cu2–O6	1.947	Cu(2)	0.485
Cu2–Cl7	2.765	Cu(2)	0.126
Cu2–Cl7	2.765	Cu(2)	0.126
$\sum s_{ij}$			2.056
Cu3–O4	2.014	Cu(2)	0.404
Cu3–O4	2.014	Cu(2)	0.404
Cu3–O5	1.993	Cu(2)	0.428
Cu3–O5	1.993	Cu(2)	0.428
Cu3–O6	2.361	Cu(2)	0.158
Cu3–O6	2.361	Cu(2)	0.158
$\sum s_{ij}$			1.980
O4–Cu1	1.99	Cu(2)	0.431
O4–Cu1	2.001	Cu(2)	0.419
O4–Cu3	2.014	Cu(2)	0.404
O4–D10	0.976	—-	—
O5–Cu1	1.984	Cu(2)	0.439
O5–Cu2	2.003	Cu(2)	0.417
O5–Cu3	1.993	Cu(2)	0.428
O5–D9	0.974	—	—
O6–Cu1	1.929	Cu(2)	0.509
O6–Cu2	1.947	Cu(2)	0.485
O6–Cu3	2.361	Cu(2)	0.158
O6–D8	0.962	—	—
Cl7–Cu1	2.742	Cu(2)	0.135
Cl7–Cu1	2.829	Cu(2)	0.106
Cl7–Cu2	2.765	Cu(2)	0.126
Cl7–D8	2.15	—	—
Cl7–D9	2.097	—	—
Cl7–D10	2.156	—	—
D8–O6	0.962	—	—
D8–Cl7	2.15	—	—
D9–O5	0.974	—	—
D9–Cl7	2.097	—	—
D10–O4	0.976	—	—
D10–Cl7	2.156	—	—

Table A.3. Selected bond angles for γ-Cu$_2$(OD)$_3$Cl at 2 K.

Angle	Degrees
Cu1–O4–Cu1	117.43(11)
Cu1–O4–Cu3	95.88(14)
Cu1–O4–D10	113.42(31)
Cu1–O4–Cu3	101.78(14)
Cu1–O4–D10	114.72(31)
Cu3–O4–D10	110.96(21)
Cu1–O5–Cu2	117.10(15)
Cu1–O5–Cu3	96.72(15)
Cu1–O5–D9	116.01(31)
Cu2–O5–Cu3	100.68(11)
Cu2–O5–D9	112.82(33)
Cu3–O5–D9	110.80(27)
Cu1–O6–Cu2	124.39(16)
Cu1–O6–Cu3	92.56(13)
Cu1–O6–D8	116.02(33)
Cu2–O6–Cu3	90.61(10)
Cu2–O6–D8	116.36(33)
Cu1–Cl7–Cu2	76.28(7)
Cu1–Cl7–D8	139.43(12)
Cu1–Cl7–D9	87.12(12)
Cu1–Cl7–D10	143.68(12)

Table B.2. Basis vectors for the space group $P\,1\,2_1/n\,1$ with $\mathbf{k}_7 = (0,\ 0,\ 0)$. The decomposition of the magnetic representation for the Cu2 site (0.5, 0, 0) is $\Gamma_{\mathrm{Mag}} = 3\Gamma_1^1 + 0\Gamma_2^1 + 3\Gamma_3^1 + 0\Gamma_4^1$. The atoms of the non-primitive basis are defined according to 1: (0.5, 0, 0), 2: (0, 0.5, 0.5). For the Cu3 site the basis vectors are the same; the positions are correspondingly 1: (0, 0, 0), 2: (0.5, 0.5, 0.5).

			BV components		
IR	BV	Atom	$m_{\|a}$	$m_{\|b}$	$m_{\|c}$
Γ_1	ψ_1	1	2	0	0
		2	−2	0	0
	ψ_2	1	0	2	0
		2	0	2	0
	ψ_3	1	0	0	2
		2	0	0	−2
Γ_3	ψ_4	1	2	0	0
		2	2	0	0
	ψ_5	1	0	2	0
		2	0	−2	0
	ψ_6	1	0	0	2
		2	0	0	2

Appendix B. Symmetry adapted magnetic structures

Table B.1. Basis vectors for the space group $P\,1\,2_1/n\,1$ with $\mathbf{k}_7 = (0,\ 0,\ 0)$. The decomposition of the magnetic representation for the Cu1 site (0.239 93, 0.767 06, 0.253 09) is $\Gamma_{\mathrm{Mag}} = 3\Gamma_1^1 + 3\Gamma_2^1 + 3\Gamma_3^1 + 3\Gamma_4^1$. The atoms of the non-primitive basis are defined according to 1: (0.239 93, 0.767 06, 0.253 09), 2: (0.260 07, 0.267 06, 0.246 91), 3: (0.760 07, 0.232 94, 0.746 91), 4: (0.739 93, 0.732 94, 0.753 09). The labeling of the representations follows the notation of Kovalev [43].

IR	BV	Atom	BV components $m_{\|a}$	$m_{\|b}$	$m_{\|c}$	IR	BV	Atom	BV components $m_{\|a}$	$m_{\|b}$	$m_{\|c}$
Γ_1	ψ_1	1	1	0	0	Γ_3	ψ_7	1	1	0	0
		2	−1	0	0			2	1	0	0
		3	1	0	0			3	1	0	0
		4	−1	0	0			4	1	0	0
	ψ_2	1	0	1	0		ψ_8	1	0	1	0
		2	0	1	0			2	0	−1	0
		3	0	1	0			3	0	1	0
		4	0	1	0			4	0	−1	0
	ψ_3	1	0	0	1		ψ_9	1	0	0	1
		2	0	0	−1			2	0	0	1
		3	0	0	1			3	0	0	1
		4	0	0	−1			4	0	0	1
Γ_2	ψ_4	1	1	0	0	Γ_4	ψ_{10}	1	1	0	0
		2	−1	0	0			2	1	0	0
		3	−1	0	0			3	−1	0	0
		4	1	0	0			4	−1	0	0
	ψ_5	1	0	1	0		ψ_{11}	1	0	1	0
		2	0	1	0			2	0	−1	0
		3	0	−1	0			3	0	−1	0
		4	0	−1	0			4	0	1	0
	ψ_6	1	0	0	1		ψ_{12}	1	0	0	1
		2	0	0	−1			2	0	0	1
		3	0	0	−1			3	0	0	−1
		4	0	0	1			4	0	0	−1

References

[1] Anderson P W 1973 *Mater. Res. Bull.* **8** 153
[2] Obradors X *et al* 1988 *Solid State Commun.* **65** 189
   Wada N *et al* 1997 *J. Phys. Soc. Japan* **66** 961
   Broholm C, Aeppli G, Espinosa G P and Cooper A S 1990
      Phys. Rev. Lett. **65** 3173
   Ramirez A P 1991 *J. Appl. Phys.* **70** 5952
[3] Ballou R, Lelièvre-Berna E and Fak B 1996 *Phys. Rev. Lett.*
      76 2125
[4] Nakamura H, Wada H, Yoshimura K and Shiga M 1988
      J. Phys. F: Met. Phys. **18** 981
[5] Wills A S and Harrison A 1996 *J. Chem. Soc. Faraday Trans.*
      92 2161
   Wills A S *et al* 1998 *Europhys. Lett.* **42** 325
   Wills A S *et al* 2000 *Phys. Rev.* B **62** R9264
   Harrison A *et al* 2000 *Physica* B **289** 217
   Wills A S *et al* 2001 *Phys. Rev.* B **64** 094436
   Dupuis V *et al* 2002 *J. Appl. Phys.* **91** 8384
   Grohol D and Nocera D G 2007 *Chem. Mater.* **19** 3061
[6] Bramwell S T and Harris M J 1998 *J. Phys.: Condens. Matter*
      10 L215
   Harris M J, Bramwell S T and Holdsworth P C W 1998
      Phys. Rev. Lett. **81** 4496
   Bramwell S T and Harris M J 2001 *Phys. Rev. Lett.* **87** 047205
   Bramwell S T and Gingrad M J P 2006 *Science* **294** 1495
[7] Stewart J R *et al* 2004 *J. Phys.: Condens. Matter* **16** L1
   Petrenko O, Lees M, Balakrishnan G and Paul D 2004
      Phys. Rev. B **70** 4
   Champion J D M *et al* 2001 *Phys. Rev.* B **64** 140407
[8] Palmer S E *et al* 2000 *Phys. Rev.* B **62** 488
[9] Wills A S *et al* 2006 *J. Phys.: Condens. Matter* **18** L37
   Bonville P *et al* 2003 *J. Phys.: Condens. Matter* **15** 7777
[10] Champion J D M *et al* 2003 *Phys. Rev.* B **68** 020401
   Poole A, Wills A S and Lelievre-Berna E 2007 *J. Phys.:*
      Condens. Matter **19** 452201
[11] Dzyaloshinsky I 1958 *J. Phys. Chem. Solids* **4** 241
   Moriya T 1960 *Phys. Rev. Lett.* **4** 228
[12] Wills A S 2001 *Phys. Rev.* B **63** 064430
   Wills A S 2001 *Can. J. Phys.* **79** 1501
   Frunzke J *et al* 2001 *J. Mater. Chem.* **11** 179
   Ballou R *et al* 2003 *J. Magn. Magn. Mater.* **262** 465
   Bisson W G and Wills A S 2008 *J. Phys.: Condens. Matter*
      20 452204
[13] Lee S H *et al* 2002 *Nature* **418** 856
   Martinho H, Moreno N O, Sanjurjo J A and Rettori C 2000
      Phys. Rev. Lett. **85** 4598
[14] Dunsiger S R *et al* 2000 *Phys. Rev. Lett.* **85** 3504
   Schiffer P *et al* 1994 *Phys. Rev. Lett.* **73** 2500
   Petrenko O A *et al* 2002 *Appl. Phys.* A **74** S760
[15] Stewart J R *et al* 2006 *J. Phys.: Condens. Matter* **19** 145291
   Stewart J R, Rainford B D, Eccleston R S and Cywinski R 2002
      Phys. Rev. Lett. **89** 186403
[16] Wills A S *et al* 2000 *Phys. Rev.* B **61** 6156
   Harrison A, Wills A S and Ritter C 1998 *Physica* B **241** 722
[17] Mirebeau I, Goncharenko I N, Dhalenne G and
      Revcolevschi A 2004 *Phys. Rev. Lett.* **93** 187204
   Cornelius A L, Light B E, Kumar R S and Eichenfield M 2005
      Physica B **359** 1243
[18] Wang R F *et al* 2006 *Nature* **439** 303
[19] Qi Y, Brintlinger T and Cumings J 2008 *Phys. Rev.* B
      77 094418
[20] Wills A S, Ballou R and Lacroix C 2002 *Phys. Rev.* B
      66 144407
[21] Shores M P, Nytko E A, Bartlett B M and Nocera D G 2005
      J. Am. Chem. Soc. **127** 13462
[22] Lee S *et al* 2007 *Nat. Mater.* **6** 853
[23] Wills A S, Raymond S and Henry J-Y 2004 *Physica* B **272** 850
[24] Zheng X G *et al* 2005 *Phys. Rev. Lett.* **95** 057201
[25] Zheng X G *et al* 2005 *Phys. Rev.* B **71** 052409
[26] Marston J B and Zeng C 1991 *J. Appl. Phys.* **69** 5962
[27] Singh R R P and Huse D A 2007 *Phys. Rev.* B **76** 180407(R)
[28] Singh R R P and Huse D A 2008 *Phys. Rev.* B **77** 144415
[29] Yang B-J, Ki Y B, Yu J and Park K 2008 *Phys. Rev.* B
      77 224424
[30] Lawler M J, Fritz L, Kim Y B and Sachdev S 2008
      Phys. Rev. Lett. **100** 187201
[31] Wiebe C *et al* 2005 *J. Phys.: Condens. Matter* **17** 6469
   Wills A S *et al* 1999 *Chem. Mater.* **11** 1936
[32] Greedan J E *et al* 1998 *Chem. Mater.* **10** 3058
   Wills A S, Raju N P and Greedan J E 1999 *Chem. Mater.*
      11 1510
   Greedan J E *et al* 2002 *Phys. Rev.* B **65** 184424
[33] Larson A C and Von Dreele R B 2000 General structure
      analysis system (GSAS) *Los Alamos National Laboratory*
      Report LAUR 86-748
[34] Wills A S, VaList-bond valence calculation and listing Program
      available from www.ccp14.ac.uk
[35] Oswald H R and Guentier J R 1971 *J. Appl. Crystallogr.* **4** 530
[36] Mizuno Y, Tohyama T, Maekawa S and Osafune T 1998
      Phys. Rev. B **57** 5326
[37] Tornow S, Entin-Wohlman O and Aharony A 1999
      Phys. Rev. B **60** 10206
[38] Gutierrez L *et al* 2002 *Eur. J. Inorg. Chem.* 2094
[39] Sarkar B *et al* 2007 *Chem. Eur. J.* **13** 9297
[40] Jones L F, Kilner C A and Halcrow M A 2007
      Polyhedron **26** 1977
[41] Wills A S 2000 *Physica* B **276** 680
   Wills A S SARA*h*—simulated annealing and representational
      analysis Program available from www.ccp14.ac.uk
[42] Wills A S 2002 *Appl. Phys.* A **74** S856
[43] Kovalev O V 1993 *Representations of the Crystallographic*
      Space Groups 2 edn (London: Gordon and Breach) These
      have been recently verified and put forward as a reliable
      source [44].
[44] Davies Z and Wills A S 2008 *J. Phys.: Condens. Matter*
      20 104232
[45] Wigner E P 1959 *Group Theory and its Application to the*
      Quantum Mechanics of Atomic Spectra
      (London: Academic)
[46] Bradley C J and Cracknell A P 1972 *The Mathematical Theory*
      of Symmetry in Solids (Oxford: Clarendon)
[47] Bertaut E F 1962 *J. Appl. Phys.* **33** 1138
   Bertaut E F 1968 *Acta Crystallogr.* A **24** 217
   Bertaut E F 1971 *J. Physique Coll.* C1 462
   Bertaut E F 1981 *J. Magn. Magn. Mater.* **24** 267
   Izyumov Yu A, Naish V E and Ozerov R P 1991 *Neutron*
      Diffraction of Magnetic Materials (New York: Consultants
      Bureau)
   Wills A S 2001 *Phys. Rev.* B **63** 13
[48] Kim J-H, Lee S-H, Lake B, Yildrim T, Nojiri H, Kikuchi H,
      Habicht K, Qiu Y and Kiefer K 2008 *Phys. Rev. Lett.*
      191 107201